# Demonstration of Spectral Defragmentation in Flexible Bandwidth Optical Networking by FWM

David J. Geisler, *Student Member, IEEE*, Yawei Yin, *Member, IEEE*, Ke Wen, Nicolas K. Fontaine, *Member, IEEE*, Ryan P. Scott, *Member, IEEE*, Shuo Chang, and S. J. Ben Yoo, *Fellow, IEEE*

***Abstract*—Flexible bandwidth elastic optical networking is an attractive solution for efficiently matching allocated bandwidth with link demand, but suffers from inevitable spectral fragmentation. In this letter, we discuss spectral defragmentation in flexible bandwidth networks using four-wave mixing (FWM) and wavelength selective switch (WSS)-based wavelength conversion blocks. Simulations show a defragmentation degree of one (i.e., the number of defragmentation blocks equals one) results in 71% and 47% reductions in blocking probability under high offered load (680 Erlangs) and low offered load (220 Erlangs), respectively. Further reductions in blocking probability result from an increased defragmentation degree. Experimental results show spectral defragmentation over 500 GHz of bandwidth for a defragmentation degree of one, validating FWM- and WSS-based spectral defragmentation in flexible bandwidth networks.**

***Index Terms*—All-optical networks, flexible bandwidth networking, spectral defragmentation, wavelength assignment.**

## I. Introduction

THE current trends in optical fiber communications are rapidly approaching the physical capacity limit of standard optical fiber [1]. It is becoming increasingly important to efficiently utilize spectral resources wisely to accommodate the ever-increasing Internet traffic demand. Meanwhile, the rigid ITU-T frequency grid (G.649.1) restricts the granularity of bandwidth segmentation and allocation, which causes a mismatch between the allocated and requested link bandwidths. Proposed flexible bandwidth network schemes utilize many low speed orthogonal frequency division multiplexing (OFDM) subcarriers to adaptively allocate spectral resources with fine granularity to satisfy link bandwidth requests ranging from subwavelength to super-wavelength [2]. This increases network utilization by better matching between traffic demand and allocated bandwidth.

However, flexible bandwidth optical networks must satisfy dynamic connection add and drop requests over free spectral resources that inevitably fragment, thus increasing the blocking probability. Fig. 1(a) shows a scenario in which

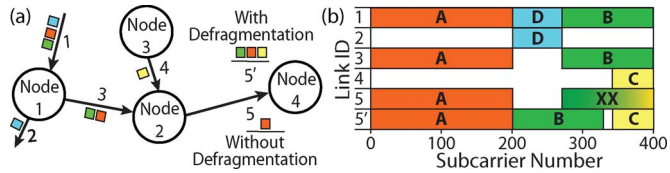


Fig. 1. (a) Flexible bandwidth networking scenario with (link 5') and without (link 5) spectral defragmentation at Node 2. Colored boxes represent successful connection requests. (b) Schematic overview of the spectral usage on each link in (a). XX indicates blocked connection requests.

connections (colored squares) from Node **2** to Node **4** (link **5**) become blocked unless spectral defragmentation is performed at Node **2** (link **5'**). Fig. 1(b) shows the corresponding spectral occupation of each link in terms of the number of OFDM subcarriers utilized. Spectral defragmentation has been investigated and achieved in the context of WDM network links by lowering connection bandwidth, (i.e., data rate) at the cost of longer transfer time [3]. However, a general solution for spectral defragmentation (i.e., aggregating free spectrum) in flexible bandwidth networks must not reduce the performance of existing connections. We propose a new approach which leverages bandwidth scalable, phase sensitive wavelength conversion based on four-wave mixing (FWM) [4] and wavelength selective switches (WSS's) to construct spectral defragmentation blocks of varying degrees (i.e., number of simultaneous defragmentation operations) to create a flexible bandwidth wavelength cross connect (FB-WXC).

In this Letter, we present a scalable FB-WXC architecture for implementing spectral defragmentation in flexible bandwidth networks and show its efficacy with an improved routing and spectrum allocation (RSA) algorithm through network simulations for various defragmentation degree capabilities. We also present a proof-of-principle experimental demonstration of spectral defragmentation over 500 GHz of optical bandwidth using a bandwidth scalable and phase sensitive wavelength conversion technique based on four-wave mixing and wavelength selective switches.

## II. Flexible Bandwidth Networking Spectral Defragmentation Simulation

Fig. 2 depicts the proposed FB-WXC architecture shown with varying defragmentation degrees ($N$) at each of $M$ inputs. At each input port, the first $1 \times N'$ WSS ($N' = N + 1$) separates incoming traffic into $N'$ spectrum blocks for defragmentation using $N$ FWM blocks. The second $N' \times 1$ WSS recombines the spectral blocks. At this point, an $M \times M$ WSS directs blocks of defragmented spectrum from each incoming link (**1**, **2** and **3**

Manuscript received May 17, 2011; revised September 08, 2011; accepted October 07, 2011. Date of publication October 13, 2011; date of current version November 29, 2011. This work was supported in part by DARPA and SPAWAR under OAWG contract HR0011–05–C–0155, by NSF ECCS Grant 1028729, and by the CISCO University Research Program.

The authors are with the Department of Electrical and Computer Engineering, University of California, Davis, CA 95616 USA (e-mail: djgeisler@ucdavis.edu).

Color versions of one or more of the figures in this letter are available online at http://ieeexplore.ieee.org.

Digital Object Identifier 10.1109/LPT.2011.2171933

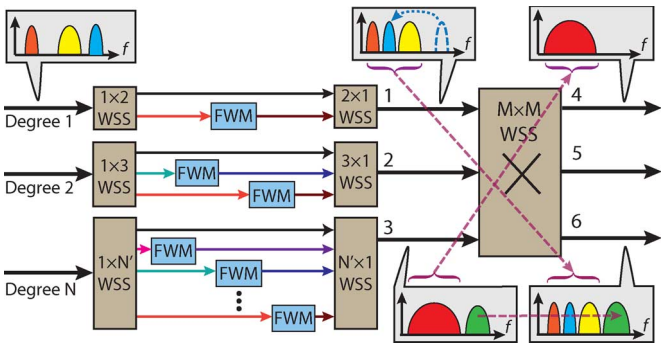


Fig. 2. Schematic of an optical spectral defragmentation capable flexible bandwidth wavelength cross connect (FB-WXC) with varying defragmentation degree $N$. $N' = N + 1$. FWM: Four-wave mixing. WSS: Wavelength selective switch.

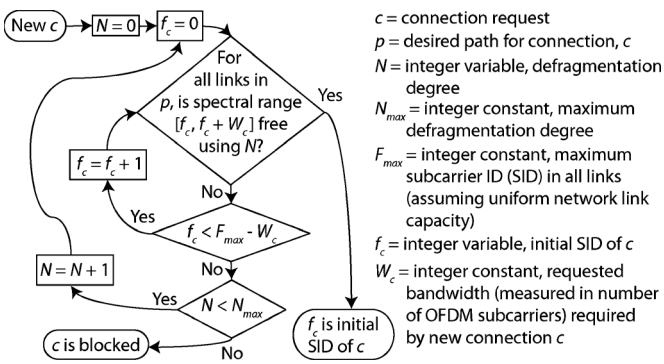


Fig. 3. Flexible bandwidth RSA algorithm with defragmentation.

in Fig. 2) to the desired output link (**4**, **5** and **6** in Fig. 2). Fig. 2 shows defragmentation at **1**, which enables spectral resources from **1** to combine with part of **3** for output on **6**. This node architecture requires that the spectrum is defragmented at **1**, **2**, and **3**, and **4**, **5**, and **6**. The amount of defragmentation necessary for a given output link can be distributed across the different input links, which reduces the number of FWM components required for each link. Simulations were used to investigate a spectral defragmentation RSA algorithm with this FB-WXC architecture in a 14-node NSFNET topology. Fig. 3 shows a block diagram of the heuristic algorithm based on a greedy search used to locate an appropriate spectrum block to accommodate the incoming bandwidth request, $c$, using a minimum of spectral defragmentation operations on path, $p$.

Network traffic was simulated using a Markov birth/death model with a Poisson distributed average request arrival rate, $\lambda$, and a negative exponential distributed average service time, $h$. Fig. 4(a) shows the blocking probability reduction for FB-WXCs for various call arrival rates, $\lambda$, as a function of degree $N$ at all node inputs. Increasing the defragmentation degree lowers the blocking probability for all $\lambda$. Fig. 4(b) shows the blocking probability for new incoming requests versus traffic load. Compared to the case of degree 0 (i.e., no defragmentation), the blocking probability for degree 1 was reduced from 0.14 to 0.04 for an offered load of 220 Erlangs, and from 0.34 to 0.18 for an offered load of 680 Erlangs.

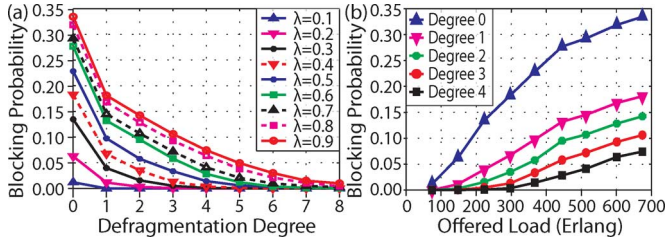


Fig. 4. (a) Blocking probability as a function of defragmentation degree ($N$) in all node input links for various call arrival rates $\lambda$. (b) Simulated blocking probability versus offered load for varying degrees of spectral defragmentation.

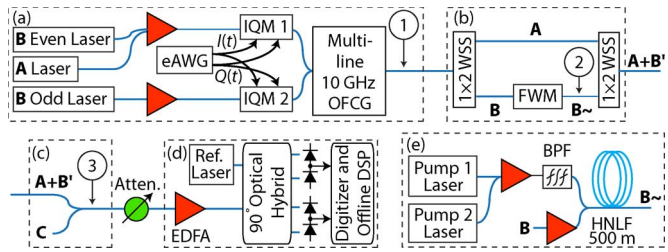


Fig. 5. FB-WXC experimental arrangement. (a) Generation of **A** and **B**, (b) spectral defragmentation, (c) addition of **C**, and (d) coherent receiver. (e) Four-wave mixing (FWM)-based wavelength conversion using two pump lasers. eAWG: Electronic arbitrary waveform generator. IQM: $I/Q$ modulator. OFCG: Optical frequency comb generator. eAWG: Electronic arbitrary waveform generator. HNLF: Highly nonlinear fiber. DSP: Digital signal processing. BPF: Bandpass filter. EDFA: Erbium-doped fiber amplifier.

## III. Experimental Demonstration

In this section, we present a proof-of-principle experimental demonstration of spectral defragmentation with degree 1 in support of future FB-WXC's. The defragmentation block was implemented using FWM [4] and WSS's to perform spectral shifting of a 200-GHz wide channel by 200 GHz. The reconfigurable bandwidth and center frequency of each WSS passband enabled filtering of unwanted FWM artifacts. The FWM process utilized two pump lasers, which provided spectral shifts equal to the frequency difference of the two pump lasers. This yielded an exact replica of the signal without the phase-conjugation that arises with single-pump FWM. Furthermore, it has been shown that FWM-based wavelength conversion is scalable to $>$ 3 THz [4] and can be used in conjunction with broadband parametric amplification [5].

Fig. 5 shows the experimental arrangement used for spectral defragmentation at Node **2** in Fig. 1. Here, channels **A**, **B**, and **C** were pseudorandom bit sequences ($2^{10} - 1$ $m$-sequence) modulated with differential phase-shifted keying (DPSK) at different rates. Respectively, the bandwidths of **A**, **B**, and **C** were 180 GHz, 180 GHz and 110 GHz, with 90 Gb/s, 180 Gb/s, and 110 Gb/s data rates. Fig. 5(a) shows how **A** and **B** were generated to create the spectra shown in Fig. 6(a). For **A**, a cw laser was amplified and then modulated with an in-phase/quadrature-phase modulator (IQM 1) to create a 4.9 Gb/s, 4.9 GHz DPSK signal. (Both IQMs were driven by a two channel, 12 GS/s electronic arbitrary waveform generator (eAWG)). **A**'s bandwidth was extended to 180 GHz by replicating the signal using a multiline 10 GHz optical frequency comb generator (OFCG), to create 18 copies within $-10$ dB, at a 10 GHz frequency spacing [6]. Channel **B** was generated from two cw lasers (Even and

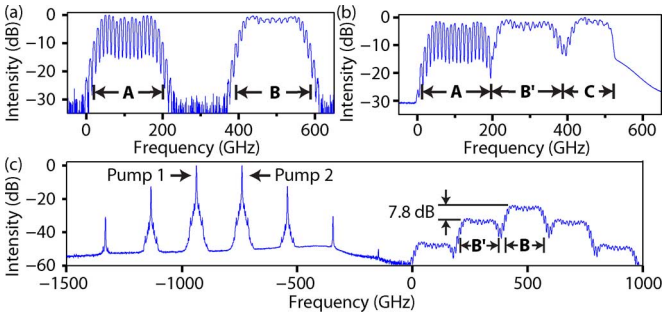


Fig. 6. Spectra (a) at point 1 showing $\mathbf{A}$ and $\mathbf{B}$ before spectral defragmentation, (b) at point 3 after spectral defragmentation showing $\mathbf{A}$, $\mathbf{B}'$, and $\mathbf{C}$, and (c) at point 2 showing the FWM process. 0 GHz represents 194.32 THz.

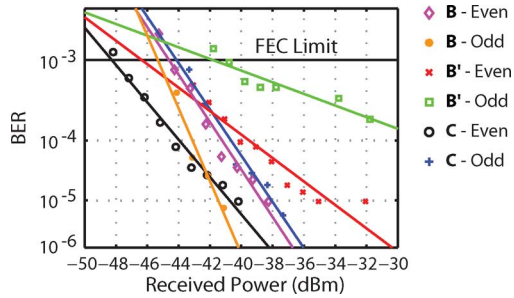


Fig. 7. BER performance of both even and odd channels for $\mathbf{B}$, $\mathbf{B}'$, and $\mathbf{C}$.

Odd) that had a 5 GHz frequency difference (and 400 GHz higher frequency than $\mathbf{A}$). They were amplified and then modulated by separate IQMs (6 GHz analog bandwidth) to generate two spectrally adjacent, but decorrelated 4.9 Gb/s carriers. Combining the even and odd DPSK signals and passing through the OFCG created 18 even and 18 odd channels for a total of 180 GHz. $\mathbf{C}$ was created by isolating 110 GHz bandwidth of $\mathbf{B}$ using an edge-pass filter.

Fig. 5(b) shows the defragmentation section which, in this case, spectrally shifts $\mathbf{B}$ by $-200$ GHz to create $\mathbf{B}'$ adjacent to $\mathbf{A}$ [see Fig. 6(b)]. This enables the addition of the new channel, C. A $1 \times 2$ WSS with 300-GHz passbands separated $\mathbf{A}$ and $\mathbf{B}$ to independent outputs with a $-40$ dB extinction ratio. Wavelength conversion was achieved using two pump lasers with 200 GHz separation, and 500 m of highly nonlinear fiber (HNLF) with a zero-dispersion wavelength at 1551 nm. Here, wavelength conversion occurs for $\mathbf{B}$ only, but in principle a WSS with many outputs and arbitrary-bandwidth wavelength conversion on each output could enable truly arbitrary spectral defragmentation. Fig. 6(c) shows the spectrum after FWM ($\mathbf{B} \sim$), which includes the two pump lasers, $\mathbf{B}$, $\mathbf{B}'$, and spectral artifacts. A second $1 \times 2$ WSS configured with 200 GHz passbands combined $\mathbf{A}$ and $\mathbf{B} \sim$ to form $\mathbf{A} + \mathbf{B}'$. The 7.8-dB power penalty on $\mathbf{B}'$ from FWM could be reduced by optimizing the HNLF or using parametric gain [5]. From a network perspective, the cost should be minimized with networking algorithms to reduce the use of defragmentation operations [7].

Fig. 5(c) shows passive combining of channel $\mathbf{C}$ with the defragmented spectrum $\mathbf{A} + \mathbf{B}'$ to form $\mathbf{A} + \mathbf{B}' + \mathbf{C}$ [Fig. 6(b)]. Fig. 5(d) shows the digital coherent receiver based on a 90° optical hybrid, balanced photodiodes, and a two-channel, 50-GS/s digitizer with 16 GHz of electrical bandwidth. Tuning the cw reference laser enabled measurements of the various channels and bit-error-rate (BER) analysis was performed offline.

Fig. 7 shows BER performance for $\mathbf{B}$, $\mathbf{B}'$, and $\mathbf{C}$ for a single even- and odd subcarrier taken at the spectral center of each channel. The BER is below the forward error correction (FEC) limit ($10^{-3}$) for each measured subcarrier, which validates this scheme for spectral defragmentation. The worst case scenario here reflects a flexible bandwidth network in which many signals or slices can have varying levels of fidelity and power differences. The power imbalance resulted in a 3-dB power penalty from the odd to even subcarrier BER results of $\mathbf{B}$. BER analysis of $\mathbf{B}'$ shows that the even subcarrier performed better than the odd subcarrier. Since the odd subcarriers were higher power (2–3 dB), the nonlinearities in the wavelength shifting process caused undesired self-phase modulation, which degraded the BER. Improving the consistency of BER measurements and also scaling $N$ would require improved power equalization prior to FWM using larger port count WSS's with pixel-by-pixel attenuation control.

## IV. Discussion and Conclusion

This Letter presents a method for solving the spectral defragmentation problem that inevitably results in flexible bandwidth networks. Simulations show that using FB-WXC's based on defragmentation blocks using FWM and WSS's resulted in a decreased blocking probability for new connection requests. Additionally, an experimental proof-of-principle demonstration of a FB-WXC with defragmentation degree 1 successfully showed spectral defragmentation over 500 GHz of optical bandwidth. Scaling to a larger defragmentation degree will enable flexible bandwidth networks to more efficiently utilize the available spectrum.

## Acknowledgment

The authors thank Nistica for the loan of the WSS units.

## References

[1] R. J. Essiambre, G. Kramer, P. J. Winzer, G. J. Foschini, and B. Goebel, "Capacity limits of optical fiber networks," *J. Lightw. Technol.*, vol. 28, no. 4, pp. 662–701, Feb. 15, 2010.

[2] M. Jinno, H. Takara, B. Kozicki, Y. Tsukishima, Y. Sone, and S. Matsuoka, "Spectrum-efficient and scalable elastic optical path network: Architecture, benefits, and enabling technologies," *IEEE Commun. Mag.*, vol. 47, no. 11, pp. 66–73, Nov. 2009.

[3] S. Naiksatam and S. Figueira, "Retrospective scheduling of elastic bandwidth reservations in lambdagrids," in *Proc. ICNS 2006*, Silicon Valley, CA, Jul. 16–18, 2006.

[4] Y. Wang, C. Yu, T. Luo, L. Yan, Z. Pan, and A. E. Willner, "Tunable all-optical wavelength conversion and wavelength multicasting using orthogonally polarized fiber FWM," *J. Lightw. Technol.*, vol. 23, no. 10, pp. 3331–3338, Oct. 2005.

[5] J. M. C. Boggio, J. D. Marconi, S. R. Bickham, and H. L. Fragnito, "Spectrally flat and broadband double-pumped fiber optical parametric amplifiers," *Opt. Express*, vol. 15, pp. 5288–5309, 2007.

[6] T. Sakamoto, T. Kawanishi, and M. Izutsu, "Asymptotic formalism for ultraflat optical frequency comb generation using a Mach–Zehnder modulator," *Opt. Lett.*, vol. 32, pp. 1515–1517, 2007.

[7] K. Wen, Y. Yin, D. J. Geisler, S. Chang, and S. J. B. Yoo, "Dynamic on-demand lightpath provisioning using spectral defragmentation in flexible bandwidth networks," in *Proc. ECOC 2011*, Geneva, Switzerland, Sep. 18–22, 2011, Paper Mo.2.K.4.